NUMERICAL PREDICTION OF NATURAL CONVECTION OCCURRING IN BUILDING COMPONENTS USING LATTICE BOLTZMANN METHOD

Frédéric Kuznik[1], Gérard Krauss[1] Gilles Rusaouen[1]

[1]Thermal Sciences Center of Lyon, UMR 5008, CNRS, INSA-Lyon, Université Lyon 1, Bât. Sadi Carnot, 20 rue de la Physique, 69100 Villeurbanne, France

ABSTRACT

A double population Lattice Boltzmann is used to solve the problem of the diffrentially heated cavity The use of a non-uniform grid makes it possible to validate the approach for laminar and transitional flows and ($10^3 \leq Ra \leq 10^8$). The results obtained, concerning the heat and mass transfers are in concordance with those of the literature. This comparison makes it possible to validate this type of approach for the prediction of anisothermal flows. To illustrate the applicability of such method for building components, the example presented is a model of solar collector.

KEYWORDS

building components, lattice Boltzmann method, double population, non-uniform mesh, natural convection.

INTRODUCTION

The numerical resolution of the Navier-Stokes equations is largely used for the prediction of the heat and mass transfers. The major difficulty lies however in the resolution of the non-linear terms present in these equations. A possible alternative lies in the use of the Boltzmann equation. Under certain assumptions, and using an adapted space-time discretization, the method becomes of Lattice Boltzmann type its application having largely been used for the study of isothermal flows (Succi 2001, Fillipova and Hanel 2000, Mey et al. 2000). The principal interest of this method lies in its complete explicit formulation and by easy parallelisation of calculations.

However, the majority of the flows, objects of engineers studies, are anisothermal. It is then possible to adapt the Lattice Boltzmann method in order to take into account the heat transfers (Chen et al. 1994, Pavlo et al. 1998, Crouse et al. 2002, Mezrhab et al. 2004). The approach with two populations, used in this article, is based on the work of He et al. 1998. It makes it possible to take into account the whole of the phenomena necessary to a correct prediction of the anisothermal flows.

In order to validate the model, we are interested in the well known case of the two dimensional cavity differentialy heated with adiabatic horizontal walls. There exists in the literature many data relating to the dynamic of the flow and heat transfer which occur in this test case (De Vahl Davis 1983, Mayne et al. 2000, Wan et al. 2001, Le Quere 1991). It is then possible to validate the model for laminar flows ($10^3 \leq Ra \leq 10^6$) and transitional flows ($10^7 \leq Ra \leq 10^8$); with respect to the flows and heat transfers

PRESENTATION OF THE MODEL

This part is devoted to a description of the model used. The complete mathematical analysis can be found in He et al. 1998. The principal assumptions are then:

- the approximation of Bhatnagar, Gross and Krook concerning the operator of collision
- the number of Knudsen is small
- the flow is incompressible
- the dissipation of heat per viscous effect is neglected.

Under these hypoyhesis, the Boltzmann equation can be written as:

$$\frac{D\tilde{f}}{Dt} = \partial_t \tilde{f} + \left(\vec{\xi}.\nabla\right)\tilde{f} = -\frac{\tilde{f}-\tilde{f}^e}{\tau_v} + F \qquad (1)$$

with $\tilde{f}$ the density distribution function, $\tilde{f}^e$ the equilibrium density distribution function of Maxwell-Boltzmann, $\vec{\xi}$ the microscopic velocity, τ_v the relaxation time and *F* external forces.
Similarly, the internal energy distribution function $\tilde{g}$ is given by the following evolution equation:

$$\frac{D\tilde{g}}{Dt} = \partial_t \tilde{g} + \left(\vec{\xi}.\nabla\right)\tilde{g} = -\frac{\tilde{g}-\tilde{g}^e}{\tau_c} \qquad (2)$$

avec τ_c the relaxation time for the internal energy distribution function.
The macroscopic variables such as density ρ, velocity $\vec{u}$ and temperature T can be calculated as the moments of the distributions functions:

$$\rho\left(\vec{x},t\right) = \int \tilde{f}\left(\vec{x},\vec{\xi},t\right)d\vec{\xi} \qquad (3)$$

$$\rho\left(\vec{x},t\right)\vec{u}\left(\vec{x},t\right) = \int \vec{\xi}\,\tilde{f}\left(\vec{x},\vec{\xi},t\right)d\vec{\xi} \qquad (4)$$

$$\rho(\vec{x},t)RT = \int \tilde{g}\left(\vec{x},\vec{\xi},t\right)d\vec{\xi} \quad (5)$$

avec R the constant of the gas.

To obtain the lattice Boltzmann model, the velocity space must be discretized: during dt , the distribution function move along the lattice link $\overrightarrow{dx_i} = \vec{c_i}dt$. In our simulations, a 9 velocities 2 dimensional (D2Q9) lattice has been used (see Figure 1). Moreover, the density f et g have been introduced by in order to avoid the implicitness of the second order scheme used to integrate the evolution equation (He et al. 1998) :

$$f = \tilde{f} + \frac{dt}{2\tau_v}\left(\tilde{f} - \tilde{f}^e\right) - \frac{dt}{2}F \quad (6)$$

$$g = \tilde{g} + \frac{dt}{2\tau_c}\left(\tilde{f} - \tilde{f}^e\right) \quad (7)$$

Figure 1 : D2Q9 model

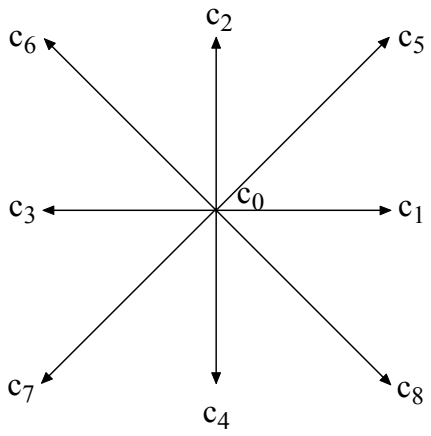

After discretization, the evolution equations become :

$$f_i\left(\vec{x}+\vec{c_i}dt, t+dt\right) + f_i\left(\vec{x},t\right) = -\frac{dt}{\tau_v + 0.5dt}\left(f_i - f_i^e\right) + \frac{dt\tau_v}{\tau_v + 0.5dt}F_i \quad (8)$$

$$g_i\left(\vec{x}+\vec{c_i}dt, t+dt\right) + g_i\left(\vec{x},t\right) = -\frac{dt}{\tau_c + 0.5dt}\left(g_i - g_i^e\right) \quad (9)$$

For the two dimensional case, applying the third-order Gauss-Hermite quadrature leads to the D2Q9 model with the following discrete velocities $\vec{c_i}$ with $i = 1...8$ and $c_0 = 0$:

$$\vec{c_i} = \left(\cos\left(\frac{i-1}{4}\pi\right), \sin\left(\frac{i-1}{4}\pi\right)\right)c \quad (10)$$

with $c = \sqrt{3RT_m}$ and T_m the mean temperature. The equilibrium density distribution function is given by:

$$f_i^e = \omega_i \rho\left[1 + 3\frac{\vec{c}_i.\vec{u}}{c^2} + 4.5\frac{\left(\vec{c}_i.\vec{u}\right)^2}{c^4} - 1.5\frac{\vec{u}^2}{c^2}\right] \quad (11)$$

with $\vec{u} = (u,v)$, $\omega_0 = \frac{4}{9}$, $\omega_i = \frac{1}{9}$ for *i=1,2,3,4* and $\omega_i = \frac{1}{36}$ for *i=5,6,7,8*.

The equilibrium internal energy density function can be written as :

$$g_0^{\ e} = -\frac{2}{3}\rho e\frac{\vec{u}^2}{c^2} \quad (12)$$

$$g_i^{\ e} = \omega_1 \rho e\left[1.5 + 1.5\frac{\vec{c}_i.\vec{u}}{c^2} + 4.5\frac{\left(\vec{c}_i.\vec{u}\right)^2}{c^4} - 1.5\frac{\vec{u}^2}{c^2}\right] \quad i = 1,2,3,4 \quad (13)$$

$$g_i^{\ e} = \omega_2 \rho e\left[3 + 6\frac{\vec{c}_i.\vec{u}}{c^2} + 4.5\frac{\left(\vec{c}_i.\vec{u}\right)^2}{c^4} - 1.5\frac{\vec{u}^2}{c^2}\right] \quad i = 5,6,7,8 \quad (14)$$

Finally, the macroscopic variables ρ , $\vec{u}$ and T can be calculated using:

$$\rho = \sum_i f_i \quad (15)$$

$$\rho\vec{u} = \sum_i \vec{c_i} f_i - \frac{dt}{2}\vec{G} \quad (16)$$

$$\rho e = \rho RT = \sum_i g_i \quad (17)$$

where $\vec{G}$ the external force acting per unit mass.

Using a Chapman-Enskog expansion, the Navier-Stokes equations can be recovered with the described model. The kinematic viscosity and the thermal diffusivity are then related to the relaxation times by:

$$\nu = \frac{\tau_v c^2}{3} \quad (18)$$

$$\chi = \frac{2\tau_c c^2}{3} \quad (19)$$

BUOYANCY FORCE AND DIMENSIONLESS PARAMETER

To demonstrate the validity of the thermal lattice Boltzmann approach proposed, simulations on the square cavity are hold, as a model of a room. This test-case is described figure 2.

Figure 2 :Differentially heated cavity

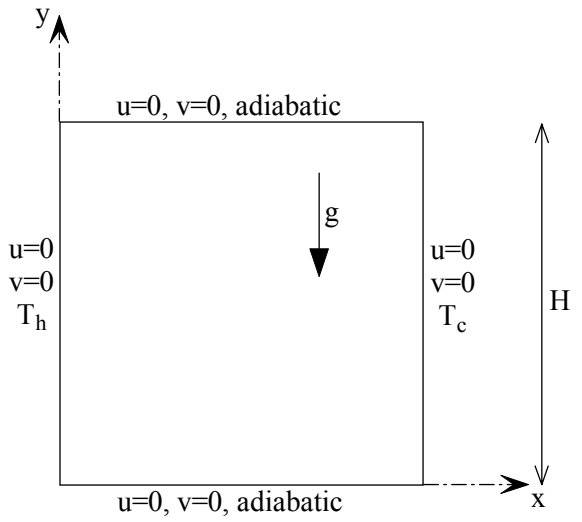

With the Boussinesq approximation, all the fluid properties are considered as constant, except the body force term in the Navier-Stokes momentum equation where the fluid density is given by:

$$\rho = \rho_m \left(1 - \beta\left(T - T_m\right)\right) \quad (19)$$

where ρ_m is the average fluid density, T_m the average fluid temperature and β the thermal coefficient expansion of the fluid. In that case, the external force acting per unit mass $\vec{G} = -\rho\beta\left(T - T_m\right)\vec{g}_r$, and the external force appearing in equation (1) is given by:

$$F_i = \frac{3\vec{G}.\left(\vec{c}_i - \vec{u}\right)}{c^2} f_i^e \quad (20)$$

The major control parameter of the test-case is the Rayleigh number given by:

$$R_a = \frac{\beta g\left(T_h - T_c\right)H^3 P_r}{\nu^2} \quad (21)$$

All the velocities are normalized using the diffusion velocity $v^* = \frac{\nu P_r}{H}$. The temperatures are dimensionless parameters using $\frac{T - T_c}{T_h - T_c}$. The dimensions are normalized using H .

IMPLEMENTATION ON NON-UNIFORM GRID

In traditional LBM, the grid is defined as a regular lattice with equal spaces. But for high Rayleigh number flows, the thermal boundary layer is very thin and then required of considerable number of nodes, wasting computational time and memory size. The Taylor series expansion - and least square - based lattice Boltzmann method (TLLBM) of Shu et al. 2001 is based on the fact that distribution functions are continuous functions in the physical space and can be defined in any mesh system: it allows mesh refinement near the walls. Even if this method is in theory meshless, we use a based non-uniform grid in order to have a more simple algorithm script.

BOUNDARY CONDITIONS

Velocity

Implementation of boundary conditions is very important for the simulation. The unknown distribution functions pointing to the fluid zone at the boundaries nodes must be specified. Concerning the no-slip boundary condition, the bounce-back rule of the non-equilibrium distribution function developed by Zou and He 1997 is used. The unknown density distribution functions at the boundary can be determined by the following condition:

$$f_\alpha - f_\alpha^{\,e} = f_\beta - f_\beta^{\,e} \quad (22)$$

where $\overrightarrow{e_\alpha}$ and $\overrightarrow{e_\beta}$ have opposite directions, $\overrightarrow{e_\alpha}$ being the direction where the distribution function is unknown and $\overrightarrow{e_\beta}$ the direction of the known distribution function. To reinforce the no-slip boundary condition, the velocity at the wall is used in the calculation of the density equilibrium functions.

Temperature

The vertical walls have constant temperatures. The condition on the adiabatic horizontal walls is converted into a Dirichlet boundary condition using a second order finite-difference approximation.

Similarly, the internal energy distribution functions can be determined with the following condition:

$$g_\alpha - g_\alpha{}^e - \overrightarrow{e_\alpha}^2\left(f_\alpha - f_\alpha{}^e\right) = g_\beta - g_\beta{}^e - \overrightarrow{e_\beta}^2\left(f_\beta - f_\beta{}^e\right) \quad (23)$$

The wall temperatures are used for the calculation of the internal energy equilibrium functions.

NUMERICAL SIMULATION

The program has been written in C, using numerical methods coming from Press et al. 1992.

The simulations are held for Rayleigh numbers from 10^3 to 10^8. The convergence criterion for all the cases tested is:

$$\max_{mesh}\left|\sqrt{\left(u^2+v^2\right)^{n+1}} - \sqrt{\left(u^2+v^2\right)^{n}}\right| \le 10^{-7} \quad (24)$$

$$\max_{mesh}\left|T^{n+1} - T^{n}\right| \le 10^{-7} \quad (25)$$

RESULTS

The comparisons with the literature results are held for $10^3 \le R_a \le 10^8$ and $P_r = 0.71$. Among the characteristic numerical values of the flow, the comparisons concern the average Nusselt number at the hot wall, the maximum horizontal velocity and the maximum vertical velocity, with the positions where they occur.

The local Nusselt number at the hot wall, is calculated via:

$$Nu_0(y) = -\frac{1}{T_h - T_c}\left.\frac{\partial T}{\partial x}\right|_{hot\ wall} \quad (26)$$

The averagel Nusselt number at the hot wall, is calculated via:

$$\overline{Nu_0} = \int_0^1 Nu_0(y)\,dy \quad (27)$$

The maximum horizontal velocity $u_{\max}$ is obtained for $y = 0.5$ at $x_{\max}$; the maximum vertical velocity $v_{\max}$ is given at $x = 0.5$ and $y_{\max}$.

Grid dependence

The grid dependence study of the results if examined before the comparisons. The case $R_a = 10^6$ has been chose. Three grid size have been tested and the results are summarized in table 1. These results show that there is no much improvement in the results when the mesh size increases from 128 to 160.

Table 1 : $R_a=10^6$

	96x96	***128x128***	***160x160***	**De Vahl Davis 1983**
u_{max}	61.627	64.133	65.831	64.630
y_{max}	0.864	0.860	0.860	0.850
v_{max}	218.92	220.54	220.79	219.36
y_{max}	0.038	0.038	0.038	0.038
$\overline{Nu_0}$	8.746	8.792	8.799	8.817

Table 2 : $10^3 \le R_a \le 10^6$

		$R_a=10^3$	**$R_a=10^4$**	**$R_a=10^5$**	**$R_a=10^6$**
u_{max}	article	3.636	16.167	34.962	64.133
	De Vahl Davis 1983	3.649	16.178	34.730	64.630
	Mayne et al. 2000	3.649	16.179	34.774	64.691
y_{max}	article	0.809	0.821	0.854	0.860
	De Vahl Davis 1983	0.813	0.823	0.855	0.850
	Mayne et al. 2000	0.812	0.823	0.853	0.846
v_{max}	article	3.686	19.597	68.578	220.537
	De Vahl Davis 1983	3.697	19.617	68.590	219.360
	Mayne et al. 2000	3.696	19.612	68.692	220.833
$Xmax$	article	0.174	0.120	0.067	0.038
	De Vahl Davis 1983	0.178	0.119	0.066	0.038
	Mayne et al. 2000	0.179	0.119	0.066	0.038
$\overline{Nu_0}$	article	1.117	2.246	4.518	8.792
	De Vahl Davis 1983	1.117	2.238	4.509	8.817
	Mayne et al. 2000	-	-	-	-

From grid dependence studies, the following grid size have been chose:

- for $R_a = 10^3$, 64x64 with uniform grid,
- for $R_a = 10^4$, 128x128 with uniform grid,
- for $R_a = 10^5$, 128x128 with non-uniform grid (which requires 200x200 with uniform grid),
- for $R_a = 10^6$, 128x128 with non-uniform grid (which requires 250x250 with uniform grid),
- for $R_a = 10^7$, 256x256 with non-uniform grid (which requires 510x510 with uniform grid),
- for $R_a = 10^8$, 256x256 with non-uniform grid (which requires 1150x1150 with uniform grid).

Numerical results

Table 2 reports the average Nusselt number at the hot wall, the maximum vertical velocity, the maximum horizontal velocity and the positions where they occur obtained for laminar flows $10^3 \leq R_a \leq 10^6$. The results obtained are close to those of the literature coming from modelings based on the Navier-Stokes equations.

Figure 3 : Isotherms $10^3 \leq R_a \leq 10^6$

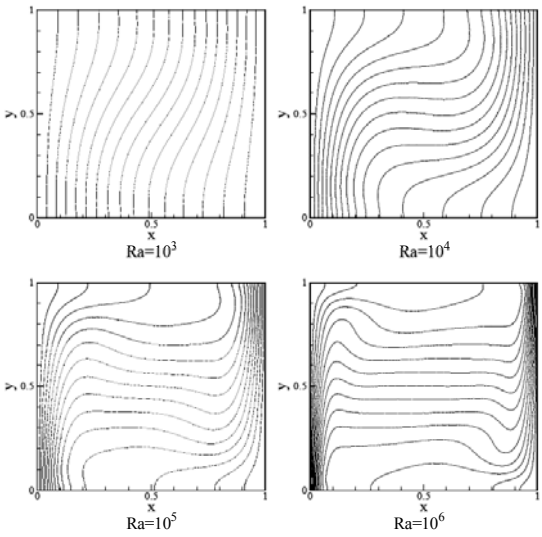

The figures 3 and 4 show respectively the isotherms and streamlines for the laminar flow cases. As the Rayleigh number increases, the fluid motion mainly takes place near the differentially heated walls and the flow in the core of the cavity becomes quasi-motionless: these flow features are well captured by the numerical method proposed.

Figure 4 :Streamlines $10^3 \leq R_a \leq 10^6$

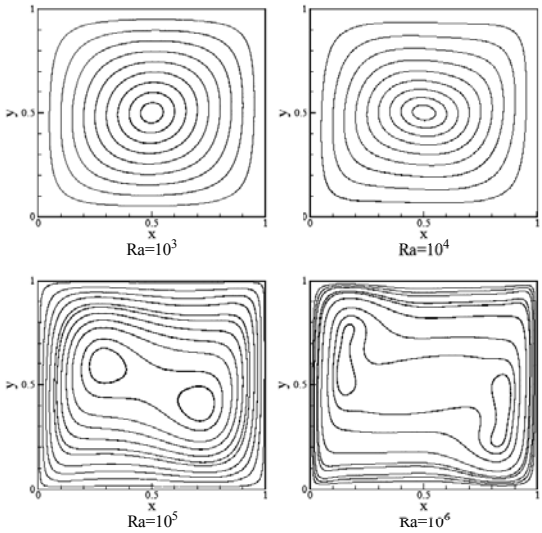

Figure 5 : Isotherms (left)andt streamlines (right) $10^7 \leq R_a \leq 10^8$

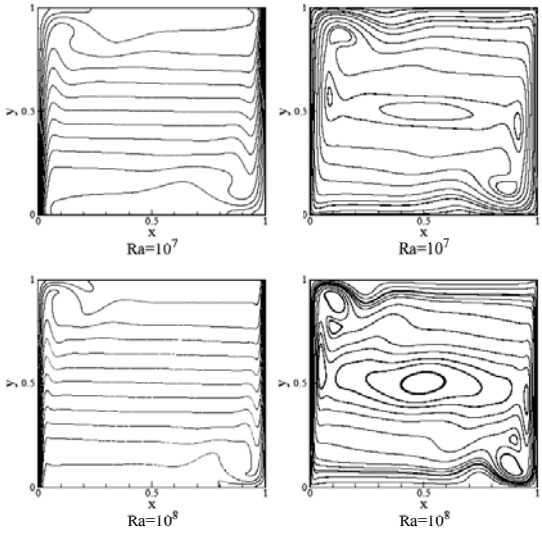

One of the main interest of this paper, is to prove that the transitional flow can be simulated using lattice Boltzmann method with non-uniform mesh at a low computational cost. The table 3 summarizes the numerical values of average Nusselt number at the hot wall, the maximum vertical velocity, the maximum horizontal velocity and the positions where they occur obtained for transitional flows $10^7 \leq R_a \leq 10^8$. From this table, the numerical values are in good agreement with those from literature.

The isotherms and streamlines for the transitional flow are shown figure 5. The temperature field is becoming more and more stratified, with horizontal streamlines. Moreover, reversed flows occur at upper-left and bottom-right corners, destabilizing the laminar flow: the transitional flow features are well captured by our model.

Table 3 : $10^7 \leq R_a \leq 10^8$

		$R_a=10^7$	$R_a=10^8$
u_{max}	article	148.768	321.457
	Wan et al. 2001	145.06	295.67
	Le Quere 1991	148.58	321.88
y_{max}	article	0.881	0.940
	Wan et al. 2001	0.92	0.94
	Le Quere 1991	0.879	0.928
v_{max}	article	702.029	2243.36
	Wan et al. 2001	714.47	2259.08
	Le Quere 1991	699.24	2222.39
x_{max}	article	0.020	0.012
	Wan et al. 2001	0.021	0.012
	Le Quere 1991	0.021	0.012
$\overline{Nu_0}$	article	16.408	29.819
	Wan et al. 2001	13.86	23.67
	Le Quere 1991	16.523	30.225

INCLINED SOLAR COLLECTOR

The second exemple of the method application concerns situations of lows occuring in solar collectors. The physical model is then a cavity (H/L=4) inclined with an angle of 45°, Pr=0.71. The model is shown figure 6. The figures 7, 8, 9 and 10 show the isotherms and streamlines obtained for Rayleigh numbers, based on the cavity width L, of $R_a=10^3$, $R_a=10^4$, $R_a=10^5$ and $R_a=10^6$.

Figure 6 : Solar collector modeling

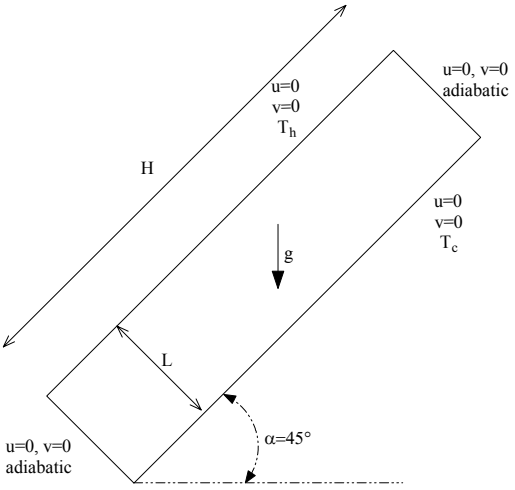

Figure 7 : Isotherms (left) and streamlines (right) for the case $R_a=10^3$

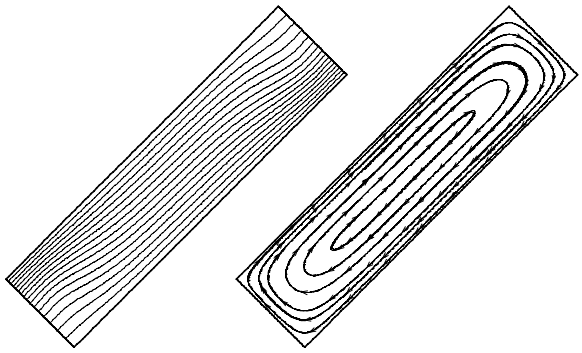

Figure 8 : Isotherms (left) and streamlines (right) for the case $R_a=10^4$

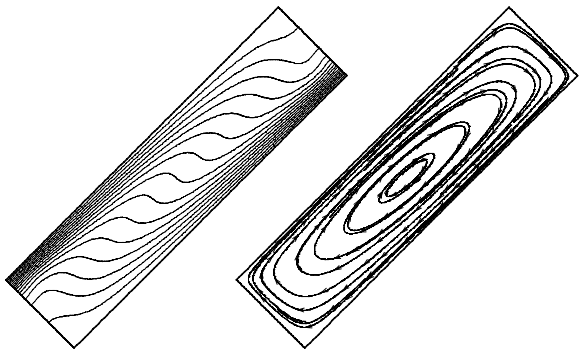

Figure 9 : Isotherms (left) and streamlines (right) for the case $R_a=10^5$

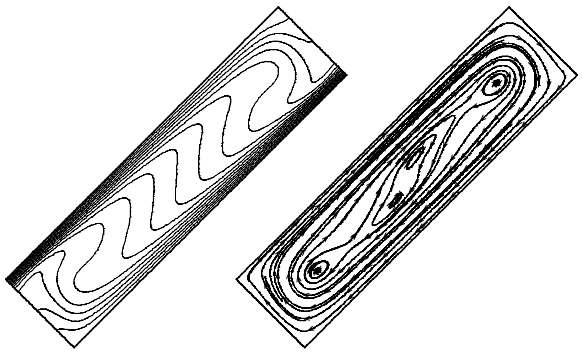

Figure 10 : Isotherms (left) and streamlines (right) for the case $R_a=10^6$

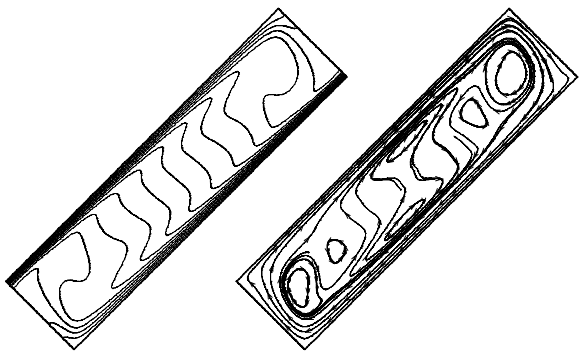

CONCLUSIONS

A thermal lattice Boltzmann model with non-uniform grid implementation has been discussed. Compare with previous studies, the TLLBM allows to reduce the mesh grid necessary to solve the Boltzmann problem. Moreover, the double population approach has shown its capability to solve heat transfer problems of building physics for laminar and transitional flows.

The lattice boltzmann method can be used to predict forced covection flows. The main problem for these simulations of fluid flows is the modelling of turbulence. The next step of our work is to introduce, in the lattice Boltzmann method described in this paper, a Large Eddy Simulation modelling of turbulence (Chen et al. 2003). The turbulent dissipative effects are then interpreted as an eddy viscosity associated to a turbulent relaxation time calculated with the help of a lattice Boltzmann stress tensor.

NOMENCLATURE

Symbols:

c_i particle discrete speed, m/s

dt time step, S

dx mesh size, m

f density distribution function, kg/m 3

g energy distribution function, J/m 3

g_r gravity, m/s²

H size of the cavity, m

N_u Nusselt number

P_r Prandtl number

R_a Rayleigh number

T temperature, K

(x,y) coordinates, m

(u,v) speed, m/s

Greek:

β thermal coefficient of expansion

ν kinematic viscosity, m²/s

χ thermal diffusivity, m²/s

ρ density, kg/m 3

τ relaxation time, S

Indices/Exponents:

e equilibrium

max maximum

REFERENCES

Succi S., The Lattice Boltzmann – For Fluid Dynamics and Beyond, Oxford University Press, 288p., (2001).

Fillipova O. and Hanel D., A Novel BGK Approach for Low Mach Number Combustion, J. Comput. Phys.,vol. 158, pp. 139-160, (2000).

Mey R., Shyy W., Yu D., and Luo L.S., Lattice Boltzmann Method for 3-D Flows with Curved Boundary, J. Comput. Phys., vol. 161, pp. 680-699, (2000).

Chen Y., Ohashi H., and Akiyama M.A., Thermal Lattice Bhatnagar-Gross-Krook Model Wuthout Nonlinear Deviations in Macrodynamic Equations, Phys. Rev. E, vol. 50, pp. 2776-2783, (1994).

Pavlo P., Vahala L., and Soe M., Linear-Stability Analysis of Thermo-Lattice Boltzmann Models, J. Comp. Phys., vol. 139, pp. 79-91, (1998).

Crouse B., Krafczyk M., Kuhner S., Rank E, and Van Treeck C., Ondoor Air Flow Analysis Based on Lattice Boltzmann Methods, Energy and Buildings, vol. 34, pp. 941-949, (2002).

Mezrhab A., Bouzidi M., and Lallemand P., Hybrid Lattice-Boltzmann Finite-Difference Simulation of Convective Flows, Computers & Fluids, vol. 33, pp. 623-641, (2004).

He X., Chen S., and Doolen G.D., A Novel Thermal Model for the Lattice Boltzmann Method in Incompressible Limit, J. Comp. Phys., vol. 146, pp. 282-300, (1998).

De Vahl Davis 1983 De Vahl Davis G., Natural Convection of Air in a Square Cavity: a Benchmark Numerical Solution, Int. J. Numer. Meth. Fluids, vol. 3, pp. 249-264, (1983).

Mayne D.A., Usmani A.S., and Crapper M., h-adaptative Finite Element Solution of High Rayleigh Number Thermally Driven Cavity Problem, Int. J. Numer. Meth. Heat Fluid Flow, vol. 10, pp. 598-615, (2000).

Wan et al. 2001 Wan D.C., Patnaik B.S.V., and Wei G.W., A New Benchmark Quality Solution for the Buoyancy-Driven Cavity by Discrete Singular Convolution , Numer. Heat Transfer B, vol. 40, pp. 199-228, (2001).

Le Quere 1991 Le Quere P, Accurate Solutions to the Square Thermally Driven Cavity at High Rayleigh Number, Computers and Fluids, vol. 20, pp. 29-41, (1991).

Shu C., Chew Y.T., and Niu X.D., Least Square-Based LBM: a Meshless Approach for

Simulation of Flows with Complex Geometry, Phys. Rev. E, vol. 64, pp. 1-4, (2001).

Zou Q. and He X., On Pressure and Velocity Boundary Conditions for the Lattice Boltzmann BGK Model, Phys. Fluids, vol. 9, pp. 1591-1598, (1997).

Press W.H., Teukolsky S.A., Vatterling W.T., and Flannery B.P., Numerical Recipes in C – The Art of Scientific Computing, Cambridge University Press, Second Edition, 994p., (1992).

Barakos G., Mitsoulis E., and Assimacopoulos D., Natural Convection in a Square Cavity Revisited: Laminar and Turbulent Models with Wall Functions, Int. J. Numer. Meth. Fluids, vol. 18, pp. 695-719, (1994).

Chen H., Kandasamy S., Orszag S., Shock R., SUCCI, S., and Yakhot V., Extended Boltzmann Kinetic Equation for Turbulent Flows, Science, vol. 301, pp. 633-636, (2003).